Received: 12 November 2021 | Accepted: 19 June 2022

DOI: 10.1111/srt.13190

ORIGINAL ARTICLE

WILEY

Evaluation of a new connected portable camera for the analysis of skin microrelief and the assessment of the effect of skin moisturisers

Sarah Gougeon[1] | Elsa Hernandez[2] | Nathalie Chevrot[2] | Thibault Vergne[1] | Marie Cherel[1] | Elodie Prestat-Marquis[1] | Matthieu Jomier[1] | Elodie Burty-Valin[2]

[1]Newtone Technologies, Lyon, France

[2]Seppic, Paris, France

Correspondance
Elodie Prestat-Marquis, Newtone Technologies, 13 Bis Place Jules Ferry, 69006 Lyon, France.
Email: eprestat@newtone.fr

Funding information
Newtone Technologies and Seppic

Abstract

Background: Silicone replicas and non-contact methods are effective methods to analyse the micrometric scale of the skin microrelief. Yet, they imply data capture in research facilities. The capabilities of a new connected portable camera were evaluated to analyse microrelief under nomadic conditions, also studying the effect of moisturisers.

Materials and methods: 3D depth maps were constructed using shape-from-shading algorithms. Roughness heterogeneity (Spa) was computed, and skin profiles were extracted to calculate roughness amplitude (Ra, Rq), as well as furrows/plateaus characteristics. Validation of the connected camera was performed on tanned cowhide leather and on the inner forearm skin of a single subject. The forearms of 18 subjects (23–60 years old) were also evaluated. While living their regular life, they self-performed triplicate acquisitions at various times. The effects of a placebo and of cream containing moisturisers—saccharide isomerate, urea or xylitylglucoside–anhydroxylitol–xylitol—were investigated, using untreated control skin as a reference.

Results: Validation of the device on leather and forearm skin shows high repeatability. The 18 subjects show the known correlation between age and changes in microrelief. While testing formulas, 8 h after a single application, all decreased Spa (−1.6/−2.1 folds). Only saccharide isomerate and xylitylglucoside–anhydroxylitol–xylitol decreased Ra (−2.4/−2.8 folds). The sectional area of plateaus was reduced from −1.5 (urea) to −2.1 folds (xylitylglucoside–anhydroxylitol–xylitol). The height of plateaus is also decreased by all moisturisers, from −1.5 (urea) to −2.1 folds (xylitylglucoside–anhydroxylitol–xylitol).

Conclusion: This novel camera device enables microrelief analysis under nomadic conditions, allowing monitoring its changes along the day and upon moisturisers' application.

KEYWORDS
3D skin imaging, connected imaging, moisturiser, nomadic imaging, roughness, skin microrelief, skin pattern

1 | INTRODUCTION

The skin surface roughness is an indicator of interest for dermatology and cosmetology. Increased in xerotic skin or irritation, it is one of the most common frequent dermatological disorders.[1–3] In addition to the discomfort triggered by dry skin, the associated roughness and unevenness degrade the appearance of the skin.[4] Yet, even a young and healthy skin presents a pattern of fine and isotropic microrelief that contributes to its resistance and to the skin's soft and velvety aspect due to the light scattering it induces.

The skin microrelief becomes clearly visible at a magnification of 5–10×. It consists of polygonal plateaus, mainly triangles or quadrangles, delineated by furrows.[5–7] These furrows are classified according to their length and depth. The only ones visible with naked eye are the primary lines, the widest and the deepest (30–100-μm deep relative to the skin surface), whereas secondary lines are shallower (5–40 μm) and narrower. This topography would mainly relate to the three-dimension organisation of the dermis and subcutaneous tissue and would reflect the functional state of the skin.[8–10] Many intrinsic and extrinsic factors influence the skin microrelief. Skin surface topography varies according to the anatomical site.[11–17] This observation not only reflects regional differences but also the effect of environmental factors such as relative humidity or UV exposure.[18–20] Changes in the topography of the skin microrelief are also induced by intrinsic ageing. With age, primary lines become deeper, whereas the number of secondary lines decreases.[21,22] As a result, the surface of the plateaus diminishes and they become anisotropic, leading to preferential structural orientations.[6]

Objective and quantitative evaluation of the skin microrelief is an essential aspect of dermo-cosmetic, especially when it comes to claims substantiation. A method of choice to analyse the microrelief is still based on skin replicas; a method that was among the very first ones developed to do so. Undirect, it takes advantage of a negative skin replica produced by smearing a silicon-based material over the skin surface. Characterisation of the topography is then performed by a contacting stylus or by optical systems, including microscopy.[23] Improvement of the method came from using a thin dyed-silicon replica and developing the Skin-Visiometer® that relies on light absorption according to the thickness of the silicone material to enable computer-assisted image analysis. Computer-assisted image analysis relies on measuring variations in light absorption according to the thickness of the dyed silicone.[19] Non-contact techniques have also been developed to directly assess the skin microrelief. One of the very first such devices is the SkinChip®, a non-optical skin capacitance imaging device taking advantage of sensors designed to recognise fingerprints.[24] It provides images of the plateaus and furrows based on the distance between the capacitive sensor and the skin microrelief detected by its hydration. This approach only provides 2D information and few data despite recent improvements in image analysis.[25] Additional quantitative data became available with the Visioscan®, a high-resolution camera taking close-up pictures of the skin under UV-A illumination. Thanks to image analysis algorithms, it computes skin topographic parameters such as smoothness, roughness and scaliness. It also analyses the anisotropy of furrows direction or the size of plateaus.[26,27] Another strategy is the 3D reconstruction of the skin topography. In that field, fringe profilometry has established itself as the technique of choice due to its accuracy and the versatility of its quantitative analysis. The technique relies on the projection of a network of fringes under different phases, in which acquisition by a camera enables the reconstruction of the skin topography.[15] The most common instruments using this approach are the PRIMOS and the DermaTOP. Another widespread instrument is the Antera 3D that reconstructs skin topography based on the shape-from-shading technology.[28] Yet, these instruments are rather designed to capture the entire face and evaluate macro-relief features such as wrinkles or fine lines than to study the genuine microrelief.[15,28]

All the above mentioned techniques have a common drawback: the obligation to perform the image acquisition in a dedicated research facility, under controlled conditions. These conditions not only include controlled temperature and humidity but also lighting and positioning which significantly differ from those encountered during regular daily life. With advances in technologies, several portable high-resolution colour cameras have been developed. They allow not only the rapid non-contact acquisition and analysis of versatile skin features: colour and complexion, lentigos, acne and so on, but also topographic features such as wrinkles, fine lines or roughness. A new connected camera, connected in real-time to data storage and analysis servers, has been specifically developed to enable acquisitions of data by the subjects themselves while living their regular daily life, which we call nomadic conditions contrary to subjects that would be required to go and/or stay in dedicated research facilities under controlled conditions (temperature, humidity *etc.*). After developing software suites, the camera and its potential in analysing the skin microrelief was evaluated under nomadic conditions. The effect of three skin moisturising ingredients on the skin microrelief was also analysed, comparing results to those obtained from the evolution of untreated control skin areas.

2 | MATERIALS AND METHODS

2.1 | Subjects

This non-invasive in vivo study was performed following the principles of the Declaration of Helsinki. It was approved by an Internal Committee in charge of in vivo studies, the medical staff and the regulatory department of Seppic (Castres, France). All subjects received detailed

information about the study, its goal and the protocol. All gave their written informed consent before enrolment.

This study took place in Paris, in February that is winter in the Northern hemisphere. It included a group of 18 healthy phototype I–IV volunteers, both men and women office workers, and presenting dry skin in the middle of the inner side of the forearm (<40 a.u.,[29] mean value of the cohort: 28.7 ± 4.4 AU) were recruited, the dryness of their skin being verified using the Corneometer CM825 (Courage+Khazaka Electronic, Köln, Germany). Their ages range between 23 and 60 years old (median age: 28.5, average age: 33.4, standard deviation [SD]: 12.1). Among others, the exclusion criteria were excessive hairiness, the presence of skin alteration or skin diseases on the inner side of the forearm and intense sun exposure during the month preceding the study. Two days before the study, the subjects were asked to stop applying any cosmetics on their forearms, clean them with water only on the morning of the study, and to avoid drinking excessively during the day of the study.

2.2 | The connected camera device

The connected camera used in this study (Newtone Technologies, Lyon, France) has been specifically designed for nomadic studies (Figure 1A). It generates its own Wi-Fi network, enabling subjects to connect to it and control it using an application on their device (smartphone, tablet or computer) thanks to a web application hosted by the camera. Study information, set up before the beginning of the study, is displayed on the connected device when acquisitions are performed (selection of subject number, time point and skin area[s]). When pictures are taken, their quality is first validated on the connected application (quality of the image, absence of external interfering light or excessive pressure—Figure 1B). They are then saved in the internal memory of the camera and uploaded to a distant server by Wi-Fi transfer.

The connected camera was initially developed to analyse features of a 25-mm diameter area of the skin. Illuminated by 12 white LED lights regularly spaced around the acquisition zone, the skin surface is captured by a high-resolution CMOS sensor with cross- or parallel-polarisation filters. Within less than 3 s, it provides skin images without polarisation filters, under cross- and parallel-polarisation. These images are recorded as 1640 × 1232 pixels RGB, JPEG fine format (lowest compression) providing a resolution of 17.6 μm/pixels.

To avoid any influence due to environmental light and its instability, especially when used in nomadic conditions, the camera is equipped with a cache that covers the illuminating LEDs, the CMOS sensor and the skin zone that is acquired. Acquisitions are performed by putting the camera cache in tight contact with the skin surface.

2.3 | Data acquisition with the connected camera

For all parts of the study performed under nomadic conditions, each subject received a connected camera and self-acquired pictures while living their regular daily life over 8 h. Prior to the study, they received training from an experimented technician who showed them how to use the camera and perform acquisition. They also had the opportunity to use it under the technician's supervision. During the study, they were asked to perform acquisitions of skin regions of their inner forearm at three different time points: at an initial time (T0, in the morning), 30 min after cream application (T30min) and after 8 h (T8h, in the late afternoon). All acquisitions were performed three times in a row, repositioning the camera between each acquisition on zones drawn with a ballpen from a template grid. These grids were just large enough to accommodate the cache of the camera, therefore enabling accurate positioning. During these 8 h, subjects were asked to avoid sport, which could result in sweating, not to wash their forearm and to avoid rubbing or scratching their forearm.

2.4 | Computation of gloss parameters

As skin specular gloss can interfere with the reconstruction of the 3D surface topography, this factor was analysed. For doing so, both RGB parallel- and cross-polarised pictures were converted into CIEL $L^*a^*b^*$ colour space. Then, the L^* channel of their difference was calculated. Further analysis focused on the central region of the image to avoid any excessive skin deformation resulting from the pressure exerted by the cache that protects the acquisition zone from external light (Figure 1D). Depending on the subject, this region corresponds to an area of 19–20 mm in diameter. From this central region in levels of grey (Figure 1D), the mean gloss was computed.

2.5 | Computation of 3D roughness parameters

If the camera enables to take pictures of the skin with all its 12 LEDs under parallel polarisation (Figure 1C), it can also light the skin with only one of its 12 LEDs resulting in highlighted shadows that depend on the skin topography. Based on this feature and the possibility to cycle between six different LEDs, skin areas illuminated from different angles were acquired. These images were used to reconstruct the raw skin texture. From there, 3D depth maps were computed using a shape-from-shading algorithm (Figure 1E).[30–32] Similarly to what was done for the analysis of gloss parameters, the analysis focused on the central region to avoid any skin deformation. The 3D depth map has the same XY resolution as 2D images (17.6 μm/pixels). It should also be noted that the height/depth of the 3D map is not absolute nor calibrated. It is expressed as a linear scale of the grey levels between black pixels that correspond to the deepest regions and the white pixels corresponding to the highest pixels. Yet, the height/depth resolution is about 20 μm and able to detect up to 3 mm.

To have an overall idea of the skin roughness, the Spa parameter, giving an insight into the heterogeneity of roughness, was first calculated using the entire 3D depth map. It corresponds to the arithmetic average of the variations in grey intensities integrated to the surface of the region analysed according to the following formula:

$$\mathrm{Spa} = \frac{1}{N} \sum_{i,j=0}^{N-1} |Z_{i,j}|$$

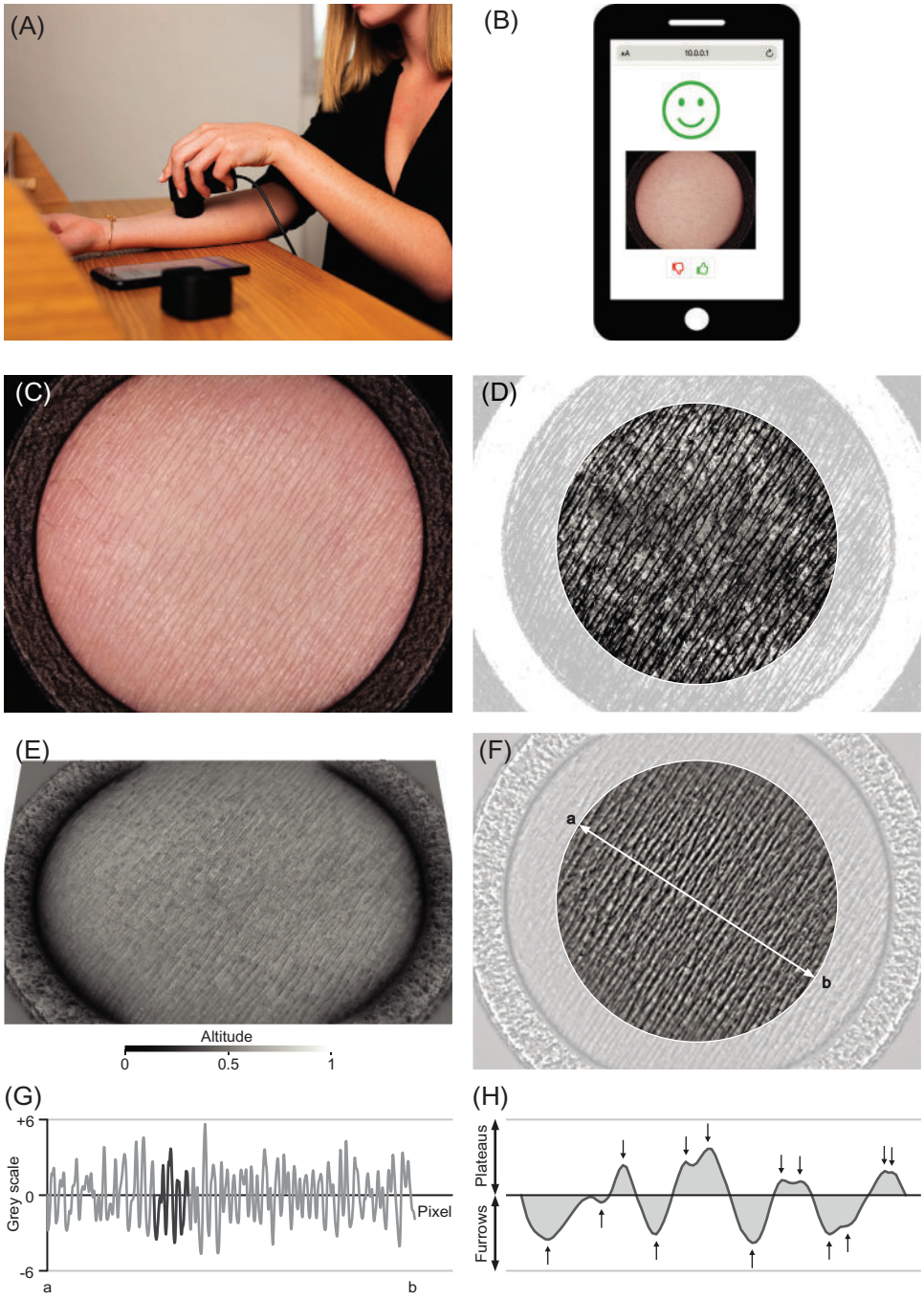

FIGURE 1 Image acquisition/treatments by the connected camera and its associated software: (A) image acquisition under nomadic conditions; (B) validation of the acquisition by the connected application; (C) raw image acquired under parallel polarisation; (D) computed gloss map and central zone of the image that is analysed; (E) reconstructed 3D depth map; (F) central region of the 3D depth map that is analysed and axis used to extract the skin profile (*a*–*b*) in the case of an anisotropic skin microrelief; (G) computed skin profile along the *a*–*b* axis, with in dark grey the region blown-up in (H); (H) details of the skin profile with arrows indicating the local minima used to calculate the number of furrows/plateaus, and, in grey, the surface used to calculate the mean area of furrows/plateaus

where Z_i corresponds to the variation between the level of grey of a pixel and the mean level of grey from all pixels analysed. N is the number of pixels in the region of interest.

3D depth maps were also used to extract skin profiles. If the axis studied has little influence on isotropic skins, it is essential in the case of anisotropic skin. Therefore, the first step was to develop an automated solution to determine the isotropy of the microrelief. If anisotropy was detected, the direction chosen to study the skin microrelief pattern parameters was perpendicular to the privileged orientation of furrows (Figure 1F). For isotropic skin, the direction used for analysis was randomly selected.

Using a skin profile (Figure 1G) extracted from the central region of the reconstructed 3D depth map, several furrow parameters were computed, considering furrows all elements of the profile with a depth below the average altitude of the profile: (1) the number of detected furrows, namely, the number of local minima in regions below the average altitude; (2) the mean depth of furrows, the mean depth of all uninterrupted regions corresponding to furrows; (3) the mean area of furrows, which is the mean sectional area of all uninterrupted regions of the profile that correspond to furrows. Similarly, plateaus parameters were computed considering only elements of the profile over the average altitude of the profile; (4) the number of detected plateaus, corresponding to the number of local maxima within regions of the profile over the average altitude; (5) the mean height of plateaus, that is, the mean height of all uninterrupted regions of the profile corresponding to plateaus; (6) the mean sectional area of plateaus: the mean area of all uninterrupted regions of the profile that correspond to plateaus.

Two additional parameters were computed based on the level of grey of the pixels from the skin profiles. They are analogous to classical roughness parameters: (7) Ra, the amplitude of the roughness defined as the arithmetic mean deviation from the mean, (8) Rq, a global measure of the amplitude of roughness, corresponding to the root-mean-square deviation from the average intensity. Ra and Rq are computed according to the following formulae:

$$\mathrm{Ra} = \frac{1}{N}\sum_{i=0}^{N-1} |Z_i|$$

$$\mathrm{Rq} = \sqrt{\frac{1}{N}\sum_{i=0}^{N-1} Z_i^2}$$

2.6 | Validation of the connected camera

To validate the ability of the connected camera to acquire roughness data and produce reliable results, a model system consisting of natural tanned cowhide leather was first tested. The inner forearm of a single phototype II subject was also analysed. Repeatability was analysed by performing five successive acquisitions without moving the camera. The influence of the positioning of the camera was also examined by performing acquisition series of the same region while rotating it by 0°, 90° and 180°, the location of the acquisition zones being outlined with a ballpen. Short-term reproducibility was determined by comparing two series of five acquisitions separated by a few minutes of interval while the camera was removed between each series.

Long-term reproducibility was tested on a silicon replica of a roughness standard. The same area was acquired in triplicate, repositioning the camera between each repetition. Acquisitions were carried out at two angles: 0° and 90°. Reproducibility was determined by comparing acquisition series performed at time points separated by 8 h.

The capacity of the connected camera to provide repeatable and reproducible skin microrelief results under the nomadic conditions used in the study was also evaluated. For this purpose, the 3D skin roughness data extracted from images self-acquired by the cohort of phototype I–IV subjects on randomly selected zones of the volar forearm were used, taking the advantage of both forearms and of the three acquisition time points (T0, T30min and T8h), each acquired in triplicate. For this analysis, 1 of the 18 subjects was excluded due to the presence of a tattoo on her right forearm, leaving 102 repetitions (17 subjects × 2 forearms × 3 time points).

TABLE 1 Composition of the vehicle cream to which 3% of the moisturisers (or water for the placebo) was added

Commercial name	INCI name	% (w/w)
Water	Aqua	85.9
Sepimax Zen™	Polyacrylate crosspolymer-6	0.1
Sepinov™ EMT 10	Hydroxyethyl Acrylate Sodium Acryloyldimethyl Taurate Copolymer	1.5
Lanol 2681	Coco caprylate/caprate	7.0
Sweet almond oil	*Prunus amygdalus dulcis* oil	1.0
Euxyl® PE 9010	Phenoxyethanol Ethylhexylglycerin	1.0
Sensiva® PA 40	Phenylpropanol Caprylyl glycol Propanediol Tocopherol	0.5

2.7 | Test of skin moisturisers

Three skin moisturising ingredients were tested on the forearm of the subjects: urea, saccharide isomerate (CAS number: 100843-69-4) and xylitylglucoside–anhydroxylitol–xylitol (CAS numbers: 101469-75-4, 53448-53-6, 87-99-0). The three ingredients were each formulated at 3% w/w in a vehicle cream, which composition is given in Table 1. The vehicle cream containing 3% of water instead of active ingredient was used as a placebo.

At the initial time (T0), volunteers used the template grid they were given before the study to draw themselves, with a ballpen, three 4 × 4 cm square zones on the inner side of both forearms. This size is large enough to accommodate and precisely position the camera device easily. On each forearm, one of the zones, selected by random draw, was left untreated. The four remaining zones of both forearms received either a placebo cream or one of the three creams with a moisturising ingredient, the positions of which were randomly selected. Subjects self-applied creams (20–30 mg sampled using a graduated spoon) by successive horizontal and vertical passes until penetration. All these procedures were explained to the subjects in a video that they received just before the study. Subjects self-acquired pictures of the six zones just before applying the cream, 30 min after and 8 h later.

Due to a tattoo on the right forearm of a subject, a set of data for the placebo and the cream containing xylitylglucoside–anhydroxylitol–xylitol had to be excluded from the analysis. Therefore, measurements from 17 subjects were considered for these two creams and the non-treated zone. Besides, before the analysis, the visual quality control of pictures was performed. This led to reject five of them (1.6% of

all acquisitions made by subjects). The excluded pictures correspond to only one of the triplicate acquisitions performed by subjects at a defined time and zone. Therefore, these were analysed using only results from duplicated acquisitions.

2.8 | Data and statistical analysis

Repeatability and reproducibility of the connected camera on the leather model system and the forearm of a single subject were assessed by calculating the mean ± SD of the coefficients of variation for colour parameters, mean gloss, roughness and microrelief parameters. The coefficients of variation were also used to compare results from triplicate measures performed at T0 and T8h on the silicon replica of a roughness standard and by the subjects under nomadic conditions. To compare these coefficients of variation between T0 and T8h, their distribution was first checked with the Shapiro–Wilk test. As none followed a Normal distribution, they were compared using the Wilcoxon–Mann–Whitney test. For this analysis, a statistical significance of 0.05 was considered.

The entire study and analyses of the experimental series on cream applications were performed blindly and randomly by both volunteers and data processors/analysts. Before analysis, results of all parameters, for all repetitions, all zones and all time points were computed. The data considered for a subject and a skin zone is the median of the triplicate acquisitions at a time point. From this, the mean ± standard error of the mean of the data from all subjects and skin zones for a time point was calculated, focusing on the evolution of parameters from T0, comparing it to the changes occurring in untreated skin zones. As a preliminary step to the statistical analysis, the normality of data distribution was verified using the Shapiro–Wilk test. In the case of a Normal distribution, homogeneity of variance was first checked using Levene's test. An analysis of variance with an analysis of maximum likelihood was then performed to determine if parameters are affected by time. When all these conditions were true, results were analysed by pairs using the Tukey method. In the case data distribution was not Normal, or variance was not homogeneous, the effect of time on parameters was studied using the non-parametric Friedman test. If validated, results from different times were compared two by two using the Nemenyi method. *p*-Values below 0.05 were considered significant.

3 | RESULTS

3.1 | Repeatability and reproducibility on a leather model system and the forearm skin of a single subject

As a preliminary step, the repeatability and reproducibility of the connected camera were analysed by studying the variability of data acquisition of the colour, gloss, roughness as well as microrelief parameters. Analysis was performed on flat model systems—a piece of natural leather and a silicon replica of a roughness standard—and, as a pilot study, on the skin of the forearm of a single subject.

On leather, the $L^*a^*b^*$ colour parameters—the closest to the RGB data captured by the CMOS sensors of the camera—show extremely high repeatability with a maximum coefficient of variation of 0.97% within acquisition series (Table 2). While including data from independent series, the L^*, a^* and b^* parameters also show extremely high repeatability with similar coefficients of variation. On this model system, computation of mean gloss and Spa, the heterogeneity of roughness, also show excellent repeatability with coefficients of variation ranging from 0.51% to 1.85% within series; up to 1.37% for Spa from independent series. Coefficients of variation calculated from 3D depth map parameters (Ra, Rq and microrelief parameters) show higher coefficients of variation, reaching up 16.32% for the sectional areas of plateaus. Yet, overall, they present a good repeatability with a variability generally slightly over 10%.

When roughness and microrelief parameters are acquired 8 h apart on the silicon replica of a roughness standard, they present low and homogeneous coefficients of variation whatever time is considered (Table 3). More importantly, the coefficients of correlation calculated from the two different times on an acquisition series (T0 and T8h) are very similar to the coefficients of variation of each time taken individually. This indicates a good reproducibility upon analysis of a stable model template.

Data acquired on the skin of the forearm show higher coefficients of variations, especially for the parameter a^*, which reaches up to 3.06% while considering acquisitions from the same series and 3.37% for independent series. Nevertheless, these levels of variation are still more than acceptable. In addition, overall mean gloss and Spa present very good repeatability with a variability of 0.70%–0.73% and 4.96%–8.14%, respectively. Similarly to the leather model system, microrelief parameters computed from 3D depth maps show lower, yet acceptable repeatability and reproducibility. Indeed, coefficients of variation range from 6.48% for Rq to a maximum of 19.01% for the repeatability of the sectional area of plateaus, 19.33% for its reproducibility.

3.2 | Repeatability and reproducibility of microrelief parameters under nomadic conditions

During this study, data were captured by the subjects themselves while living their regular daily life, which we call nomadic conditions, compared to 'classical' studies that are performed in dedicated research facilities in a controlled environment. Therefore, it was crucial to ensure that acquisitions and results were also sound under these conditions. For doing so, data of 3D roughness parameters from the acquisitions performed by 17 subjects on the untreated skin zone of their two forearms and three time points were analysed. These represent 102 series of acquisitions performed in triplicate.

Considering all series, the coefficient of variation of data from acquisitions performed at the same time, in a row, whatever time point considered, varies from a minimum of 5.38% ± 3.99% for Spa at T30min to a maximum of 14.91% ± 8.45% at T0 for the sectional area of furrows (Table 3). While comparing coefficients of variation from data acquired at different time points, only the one of Spa at T0 significantly differs

TABLE 2 Means, standard deviations and coefficients of variation from acquisition signals, mean gloss, roughness and microrelief parameters on two independent series of five repeated acquisitions and different angles

	Mean ± SD			Coefficient of variation (%)	
Parameters	**0°**	**90°**	**180°**	**Within series**	**All series**
Leather					
L^*	43.52 ± 0.07	43.40 ± 0.10	43.31 ± 0.10	0.28	0.35
	43.21 ± 0.12	43.14 ± 0.07	43.35 ± 0.09	0.30	
a^*	38.88 ± 0.09	38.97 ± 0.11	38.64 ± 0.26	0.55	0.80
	39.01 ± 0.06	38.22 ± 0.18	38.81 ± 0.18	0.97	
b^*	39.83 ± 0.06	40.03 ± 0.13	39.56 ± 0.45	0.82	0.76
	39.88 ± 0.21	39.38 ± 0.14	39.82 ± 0.10	0.69	
Mean gloss	76.22 ± 0.05	75.89 ± 0.05	74.84 ± 1.59	1.38	1.16
	76.62 ± 0.44	76.64 ± 0.44	75.99 ± 0.08	0.60	
Spa	1.43 ± 0.01	1.44 ± 0.01	1.44 ± 0.01	0.51	1.37
	1.45 ± 0.02	1.45 ± 0.04	1.44 ± 0.01	1.85	
Ra	1.66 ± 0.01	1.34 ± 0.09	1.43 ± 0.13	10.99	9.99
	1.43 ± 0.10	1.49 ± 0.17	1.39 ± 0.11	9.00	
Rq	2.09 ± 0.01	1.71 ± 0.09	1.82 ± 0.18	10.53	10.05
	1.82 ± 0.13	1.97 ± 0.24	1.75 ± 0.15	9.73	
Number of detected furrows	79.40 ± 1.34	83.00 ± 9.80	83.40 ± 7.13	8.27	8.83
	86.20 ± 9.98	82.60 ± 8.08	79.80 ± 5.54	9.60	
Depth of furrows	1.29 ± 0.03	1.10 ± 0.07	1.10 ± 0.15	11.30	10.36
	1.15 ± 0.08	1.14 ± 0.14	1.12 ± 0.13	9.60	
Sectional area of furrows	19.69 ± 0.69	16.54 ± 2.04	16.63 ± 3.08	14.30	14.94
	15.40 ± 1.56	14.97 ± 1.28	15.80 ± 2.84	12.32	
Number of detected plateaus	73.20 ± 1.92	76.40 ± 6.91	79.00 ± 7.38	7.91	8.90
	78.20 ± 6.10	86.60 ± 6.35	85.40 ± 3.51	7.62	
Height of plateaus	1.19 ± 0.02	1.02 ± 0.18	1.12 ± 0.08	11.50	11.16
	1.09 ± 0.11	1.15 ± 0.16	1.04 ± 0.08	11.16	
Sectional area of plateaus	15.61 ± 0.57	15.14 ± 4.04	16.50 ± 2.29	16.32	15.08
	14.17 ± 2.35	15.91 ± 2.76	15.31 ± 0.59	13.89	
Skin					
L^*	69.53 ± 0.18	69.69 ± 0.26	69.79 ± 0.14	0.31	0.95
	69.21 ± 0.23	68.83 ± 0.24	68.26 ± 0.87	0.93	
a^*	15.18 ± 0.25	14.41 ± 0.14	14.32 ± 0.20	2.99	3.37
	15.10 ± 0.33	14.89 ± 0.27	15.33 ± 0.67	3.06	
b^*	15.98 ± 0.13	15.83 ± 0.11	16.24 ± 0.71	2.68	2.55
	15.40 ± 0.16	15.72 ± 0.30	15.67 ± 0.14	1.57	
Mean gloss	77.14 ± 0.28	78.03 ± 0.38	77.06 ± 0.28	0.70	0.81
	76.99 ± 0.20	77.21 ± 0.10	76.19 ± 0.59	0.73	
Spa	1.24 ± 0.04	1.23 ± 0.11	1.16 ± 0.12	8.14	6.62
	1.17 ± 0.06	1.24 ± 0.05	1.22 ± 0.06	4.96	
Ra	1.37 ± 0.07	1.30 ± 0.13	1.24 ± 0.16	9.99	9.16
	1.23 ± 0.13	1.23 ± 0.11	1.26 ± 0.05	7.70	

(Continues)

TABLE 2 (Continued)

Parameters	Mean ± SD			Coefficient of variation (%)	
	0°	90°	180°	Within series	All series
Rq	1.67 ± 0.08	1.60 ± 0.15	1.53 ± 0.20	9.41	8.19
	1.52 ± 0.13	1.53 ± 0.12	1.57 ± 0.06	6.48	
Number of detected furrows	63.40 ± 4.67	67.20 ± 11.39	71.20 ± 7.53	12.47	12.64
	71.40 ± 11.26	75.20 ± 6.22	68.20 ± 9.01	12.43	
Depth of furrows	1.07 ± 0.06	1.01 ± 0.15	0.94 ± 0.15	12.93	10.87
	1.03 ± 0.09	0.97 ± 0.08	0.99 ± 0.09	8.78	
Sectional area of furrows	17.49 ± 1.16	16.46 ± 1.35	15.36 ± 2.64	11.71	10.45
	18.14 ± 0.86	16.85 ± 1.45	15.42 ± 1.07	9.35	
Number of detected plateaus	60.60 ± 5.94	64.20 ± 10.92	67.40 ± 2.88	11.55	10.91
	58.60 ± 7.40	62.20 ± 4.44	68.80 ± 3.83	10.57	
Height of plateaus	1.34 ± 0.11	1.23 ± 0.20	1.20 ± 0.22	14.43	14.57
	1.16 ± 0.19	1.12 ± 0.17	1.14 ± 0.12	13.26	
Sectional area of plateaus	18.48 ± 3.23	18.90 ± 4.43	17.33 ± 3.21	19.01	19.33
	15.52 ± 2.94	14.84 ± 1.95	16.14 ± 2.73	15.78	

TABLE 3 Means, standard deviations and coefficients of variation of roughness and microrelief parameters from a silicon replica of a roughness standard acquired using two independent series acquired at different angles (0° and 90°) with three repeated acquisitions each

Parameters	Series	Mean ± SD		Coefficient of variation (%)		
		T0	T8h	T0	T8h	T0 and T8h
Spa	0°	2.66 ± 0.06	2.60 ± 0.01	2.24	0.31	1.94
	90°	2.24 ± 0.01	2.19 ± 0.01	0.63	0.26	1.14
Ra	0°	2.66 ± 0.10	2.59 ± 0.04	3.77	1.69	2.90
	90°	2.50 ± 0.04	2.42 ± 0.09	1.46	3.69	2.98
Rq	0°	3.03 ± 0.11	2.91 ± 0.03	3.71	0.86	3.08
	90°	2.94 ± 0.05	2.80 ± 0.09	1.74	3.05	2.81
Number of detected furrows	0°	129.1 ± 11.5	102.9 ± 13.4	8.93	13.01	15.69
	90°	208.8 ± 25.3	187.4 ± 23.2	12.10	12.37	12.44
Depth of furrows	0°	2.59 ± 0.09	2.56 ± 0.05	3.51	1.85	2.60
	90°	2.19 ± 0.16	2.23 ± 0.21	7.10	9.56	7.61
Sectional area of furrows	0°	22.35 ± 0.70	21.94 ± 0.40	3.11	1.83	2.50
	90°	16.09 ± 2.64	17.53 ± 3.08	16.38	17.55	15.95
Number of detected plateaus	0°	84.2 ± 7.2	73.9 ± 7.9	8.60	10.72	11.18
	90°	189.6 ± 28.8	168.7 ± 26.8	15.19	15.91	15.30
Height of plateaus	0°	2.65 ± 0.06	2.06 ± 0.17	3.71	0.86	3.08
	90°	2.60 ± 0.02	2.15 ± 0.21	0.59	9.91	8.52
Sectional area of plateaus	0°	23.60 ± 0.58	16.35 ± 2.56	2.44	15.63	1.67
	90°	23.45 ± 0.20	17.73 ± 2.78	0.84	15.66	10.64

from those at T30min and T8h ($p = 0.0273$ vs. T30min and $p = 0.0036$ vs. T8h). For all other parameters, there are no significant differences in the coefficient of variation for acquisition series at different times.

To have an idea of the reproducibility, we also calculated the coefficients of variation of all parameters by combining data from two time points: T0 and T30min or T0 and T8h (Table 4). For all parameters, the coefficients of variation of data combining acquisitions performed at T0 and T30min lead to values almost always within the range of the coefficient of variation from data acquired at T0 or T30min alone. The only exception is the number of detected plateaus that led to values a few tenths of a percent higher. This indicates a good reproducibil-

TABLE 4 Means, coefficients of variation and their standard deviations from roughness and microrelief parameters acquired by subjects on the untreated control skin zone of their inner forearms and at three time points

	Mean ± SD			Coefficient of variation (% ± SD)				
Parameters	T0	T30min	T8h	T0	T30min	T8h	T0 and T30min	T0 and T8h
Spa	0.91 ± 0.17	0.92 ± 0.17	0.96 ± 0.17	8.67 ± 6.03	5.38 ± 3.99	5.78 ± 4.27	8.02 ± 4.29	9.36 ± 5.00
Ra	1.02 ± 0.21	1.04 ± 0.22	1.07 ± 0.22	9.91 ± 6.43	6.65 ± 4.37	8.77 ± 6.35	9.25 ± 4.40	11.13 ± 4.99
Rq	1.27 ± 0.26	1.29 ± 0.26	1.32 ± 0.26	9.34 ± 6.49	6.31 ± 4.37	8.19 ± 6.01	8.81 ± 4.44	10.67 ± 4.71
Number of detected furrows	63.73 ± 9.68	64.52 ± 6.57	63.46 ± 8.61	11.59 ± 6.15	10.29 ± 6.68	9.11 ± 4.38	11.66 ± 4.22	12.96 ± 3.34
Depth of furrows	0.83 ± 0.19	0.84 ± 0.19	0.86 ± 0.20	11.82 ± 7.44	9.39 ± 6.46	11.60 ± 8.03	11.50 ± 4.88	13.55 ± 5.90
Sectional area of furrows	12.38 ± 3.82	13.18 ± 4.32	13.12 ± 3.67	14.91 ± 8.45	12.47 ± 6.00	14.38 ± 8.72	14.42 ± 5.25	16.55 ± 5.97
Number of detected plateaus	61.71 ± 7.94	61.63 ± 6.51	61.22 ± 7.78	8.66 ± 4.88	9.07 ± 5.38	9.90 ± 4.80	8.96 ± 3.70	10.30 ± 3.30
Height of plateaus	0.92 ± 0.22	0.95 ± 0.19	0.98 ± 0.21	12.47 ± 7.79	9.71 ± 6.75	11.81 ± 7.23	12.40 ± 6.19	14.09 ± 6.82
Sectional area of plateaus	12.68 ± 3.90	13.18 ± 3.85	13.59 ± 3.65	13.06 ± 6.88	11.39 ± 5.25	12.60 ± 6.17	12.84 ± 4.81	14.21 ± 5.24

ity of all parameters within 30 min. Yet, when a similar comparison is performed 8 h apart by calculating the coefficient of variation of acquisitions performed at both T0 and T8h, the result is always a few per cent higher than those from acquisitions carried out at T0 or T8h alone—which are similar—or by combining results from acquisitions performed at T0 and T30min. Taken together, these results indicate that while skin roughness and microrelief parameters are reproducible within 30 min, they are not 8 h apart, indicating changes in skin roughness.

3.3 | Age-dependent changes in skin microrelief

To evaluate the ability of the connected camera and our approach to detect variations of the skin microrelief, the effect of a factor known for its influence was first analysed. For doing so, an analysis of Pearson correlation between the age of the subjects and the various parameters computed from the 3D depth maps was performed.

Results (Table 5) indicate that no correlation between the age of the subjects and the global 3D roughness parameter Spa exist. A significant but weak correlation is observed between ageing and increased skin roughness measured by both, Ra and Rq. Yet, ageing correlates significantly and negatively with the number of furrows and plateaus, whereas the sectional area of furrows and plateaus are positively correlated.

3.4 | Effect of skin moisturisers on skin microrelief

In a final experimental series, the impact of moisturisers on skin microrelief was evaluated. Hence, the effect on microrelief parameters of three creams, each containing a different active ingredient was monitored, comparing results to those obtained by the application of a placebo and those of an untreated control zone. As results from the cohort of subjects show variability over the 8 h of the study whereas it shows reproducibility on a model system, this indicates an evolution of skin roughness and microrelief. Therefore, the analysis focused on variations of skin parameters, taking T0 as a reference, and comparing the evolution of skin zones onto which a cream was applied to skin zones where no cream was applied.

The initial plan was to test three time points: the initial time point (just before cream application), 30 min and 8 h after applying the cream. Nevertheless, the application of a cream onto the skin can impact skin gloss that could interfere with the accuracy of the construction of 3D depth maps. Therefore, the effect of creams on the specular reflection of the skin was first checked. Compared to control areas, the application of a cream, but the one containing saccharide isomerate,

TABLE 5 Pearson coefficient of correlation between skin microrelief parameters and the age of subjects

Parameter	Correlation with age	Two-tailed probability
Spa	+0.39	0.1051
Ra	+0.48	0.0462
Rq	+0.48	0.0414
Number of detected furrows	−0.66	0.0031
Depth of furrows	+0.45	0.0626
Sectional area of furrows	+0.68	0.0021
Number of detected plateaus	−0.63	0.0054
Height of plateaus	+0.45	0.0598
Sectional area of plateaus	+0.71	0.0010

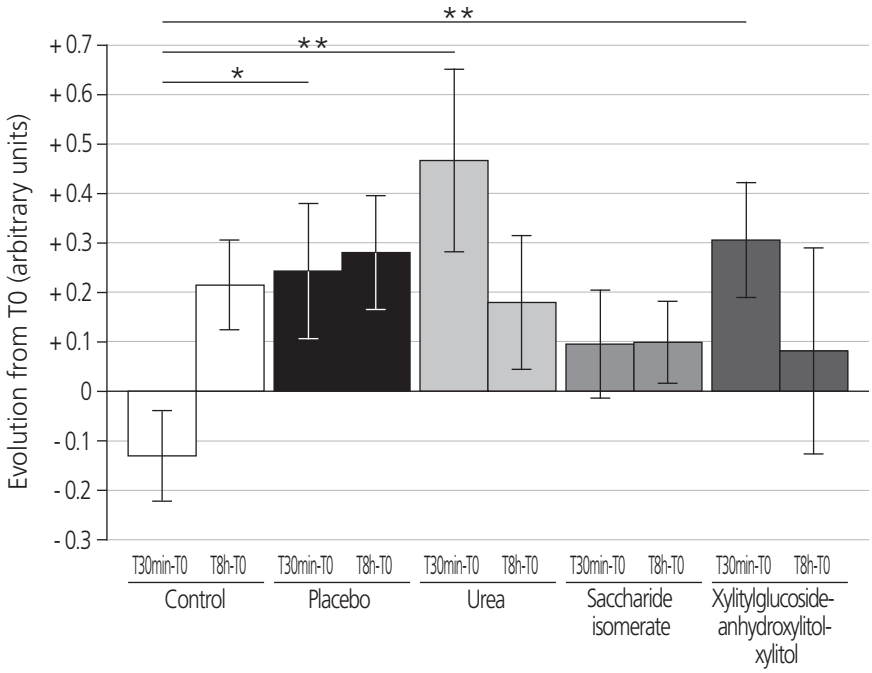

FIGURE 2 Evolution of the mean gloss parameter for untreated control zones and skin zones that received the placebo or creams containing a moisturising ingredient. Results are presented as mean ± standard error of the mean (SEM) between two time points. $^{*}p < 0.05$, $^{**}p < 0.001$

significantly increases mean gloss after 30 min (Figure 2A). This significant increase ranges from 1.7 folds for the placebo and reaches 4.6 folds for the urea-containing cream. In addition, compared to control zones, skin areas treated with the urea or the xylitylglucoside–anhydroxylitol–xylitol-containing cream show an increased gloss heterogeneity between T0 and 30 min after application: +5.0 folds when urea is the active ingredient and +4.2 folds in the case of xylitylglucoside–anhydroxylitol–xylitol (Figure 2B). As none of the mean gloss or gloss heterogeneity variations are significant between T0 and 8 h, the microrelief analysis focused on variations after the sole 8-h-time point.

On control areas, statistical analysis of microrelief parameters between T0 and 8 h shows that all of them are statistically higher, except the number of detected furrows and plateaus. These statistical differences range from $p = 0.0022$ for the sectional area of furrows to $p < 0.0001$ for Spa or the sectional area of plateaus. These results indicate a natural increase in skin microrelief roughness during the 8 h studied. Due to this evolution, the effect induced by moisturisers was analysed relatively to the evolution of the microrelief observed on untreated areas.

The variations in the heterogeneity of the skin microrelief computed from the 3D depth map show that the placebo could tend to decrease the Spa parameter compared to the control (Figure 3A). Still, only creams containing an active ingredient led to a reduction in roughness heterogeneity that was statistically significant. This decrease is within the same range whatever the active ingredient: between a minimum of −1.6 folds for the cream containing urea and a maximum of −2.1 folds when xylitylglucoside–anhydroxylitol–xylitol is the active ingredient.

Highly correlated, the Ra and Rq parameters calculated on the skin profile extracted from the 3D depth map show similar results (Figure 3B,C). Only the saccharide isomerate and the xylitylglucoside–anhydroxylitol–xylitol-containing creams induce a statistically significant decrease in the heterogeneity of the skin profile: −2.4 folds for Ra and −2.3 folds for Rq and −2.8 folds for Ra and −2.6 folds for Rq, respectively. These variations of the skin profile do not coincide with variations in the number, depth or sectional area of furrows as none of the cream induce significant changes over the 8 h-period studied (Figure 4A–C). They are also not linked to any change in the number of detected plateaus (Figure 4D). Interestingly, two parameters from the skin microrelief are significantly modified by the application of creams. The sectional area of plateaus is reduced by −1.3 (placebo) to −1.9 folds (xylitylglucoside–anhydroxylitol–xylitol) depending on the cream used. The other parameter affected is the height of plateaus. It is reduced by all creams containing an active ingredient, from −1.5 folds for urea to −2.1 for xylitylglucoside–anhydroxylitol–xylitol (Figure 4E,F).

4 | DISCUSSION

The analysis of silicone replicas and fringe projection acquisition are still gold standards to evaluate the skin microrelief. Yet, these approaches imply skilled technicians and rather bulky equipment that requires performing all acquisitions in research facilities. As studies are performed in dedicated facilities, they are generally performed under controlled conditions that can poorly represent daily life conditions. With technological advances, portable camera devices have been specifically developed to perform cosmetic studies under nomadic conditions. They became useful for claim substantiation under real-life conditions. Yet, these cameras have been essentially designed to analyse skin colour, gloss and/or visible skin textures. So far, none can study the micrometric scale of the skin microrelief.

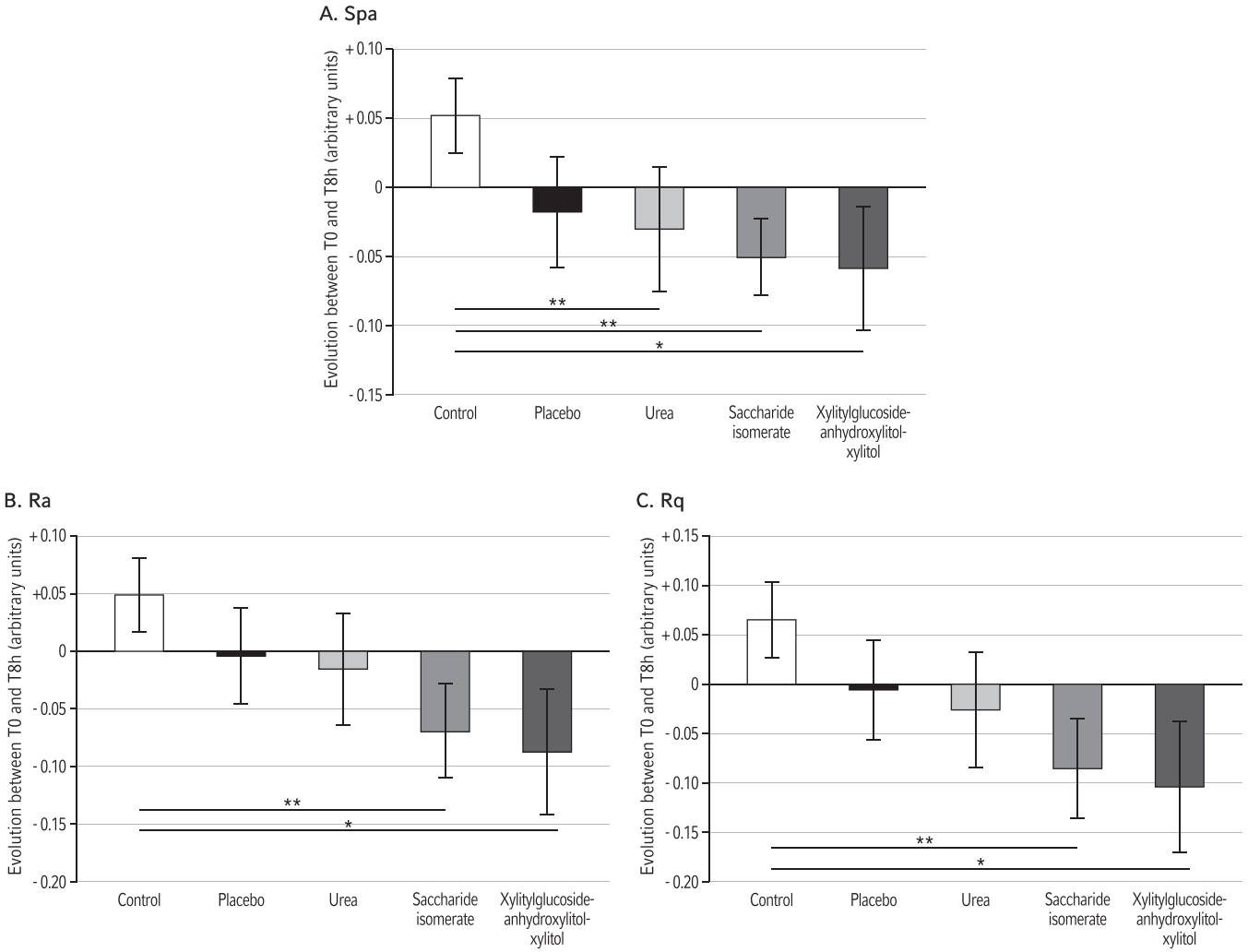

FIGURE 3 Evolution of 3D roughness parameters for untreated control zones and skin zones that received the placebo or creams containing a moisturising ingredient. (A) Spa, the heterogeneity of roughness; (B) Ra, the amplitude of roughness; (C) Rq, the global amplitude of roughness. Results are presented as mean ± standard error of the mean (SEM) between T0 and 8 h later. $^{*}p < 0.05$, $^{**}p < 0.001$

The connected camera used in this study is such a portable camera device. Taking advantage of its embedded validation application, its real-time connection to data storage servers/analysis software, and the possibility to produce images with unidirectional light from different angles, its analysis software suite was further developed to produce 3D depth maps based on a shape-from-shading approach.[30–32] This feature enables the extraction of a single skin profile, allowing the computing of skin furrows and plateaus parameters from the skin microrelief under real-life conditions.

An initial step was to ensure the reliability of acquisition/analysis. Repeatability studies of colour parameters on a leather model system and the skin of a single subject show extremely low coefficients of variations. Yet, a^* and b^* colour parameters of the skin from the phototype II subject show slightly higher values. This could be explained by the fact that such a light skin colour is characterised by relatively high L^* and quite low a^* and b^* values presenting some variability. Mathematically, low values can produce higher coefficients of variation, although not corresponding to any physical reality. Indeed, the coefficient of variation is calculated as the SD divided by the mean. When the mean approximates zero or low values, it tends to produce meaningless infinite or high values. Finally, mean gloss leads to measures presenting coefficients of variation with very low values.

Yet, the Spa parameter extracted from raw skin texture images, Ra and Rq, as well as microrelief parameters extracted from 3D depth maps show higher variability. Several factors can explain this. First, as already mentioned earlier, is the fact that the coefficient of variation is higher when computed on parameters with low values. This can be true for Ra, Rq, the depth of furrows and the height of plateaus that present particularly low values. A third factor must be considered. Whatever the exact method used, all shape-from-shading approaches use grey levels to compute the 3D depth map.[32] Therefore, they can only show very high sensitivity to minute changes in lighting of the raw skin texture images. Besides, the pictures used for the 3D reconstruction were acquired under parallel polarisation, which renders them extremely sensitive to any change in specular gloss.[33] This is the reason why skin gloss was also studied. This also explains why, 30 min after the appli-

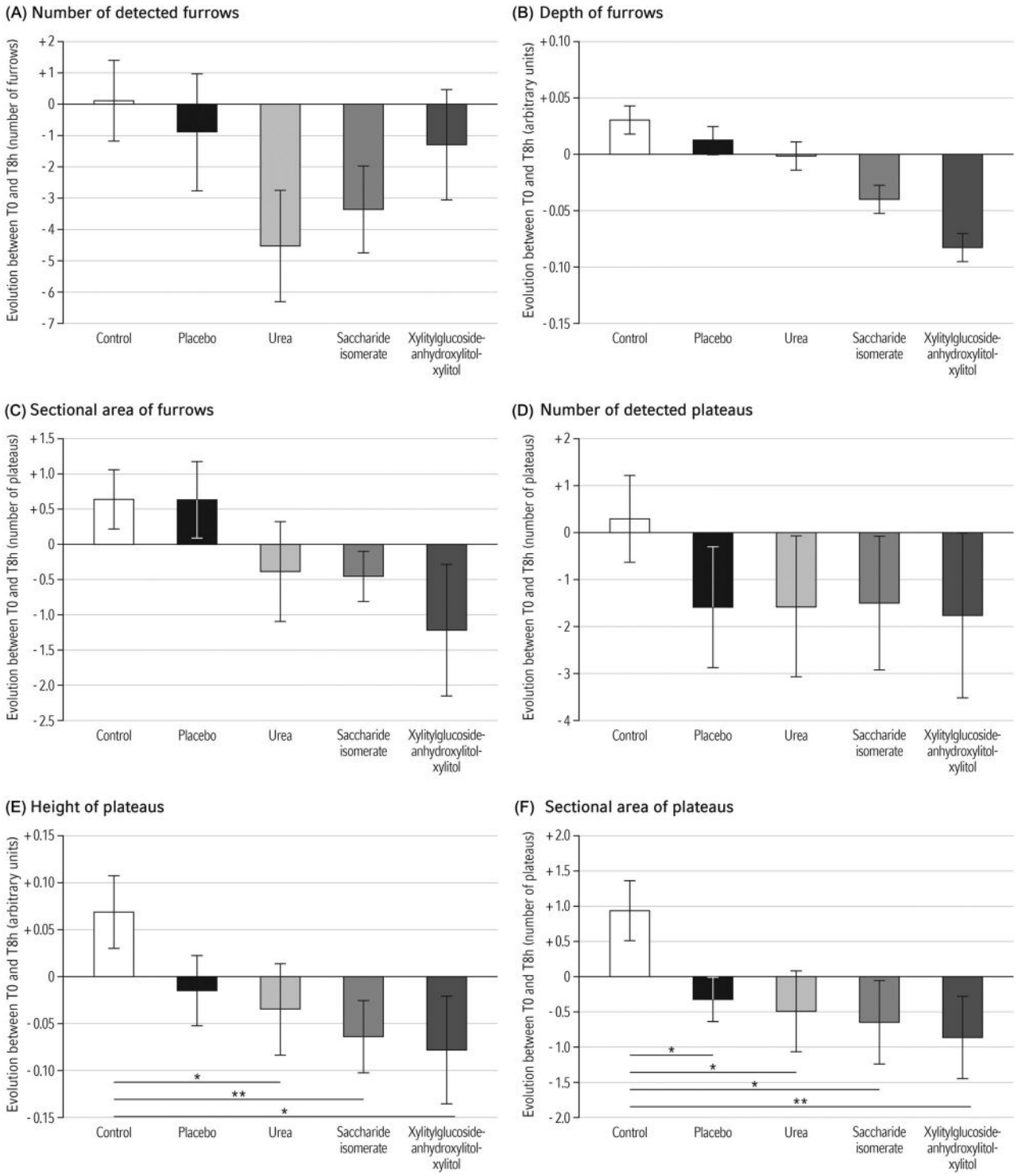

FIGURE 4 Evolution of microrelief parameters for untreated control zones and skin zones that received the placebo or creams containing a moisturising ingredient. (A) the number of detected furrows; (B) the depth of furrows; (C) the sectional area of furrows; (D) the number of detected plateaus; (E) the height of plateaus; (F) the sectional area of plateaus. Results are presented as mean ± standard error of the mean (SEM) between T0 and 8 h later. $^{*}p < 0.05$, $^{**}p < 0.001$

cation of creams, microrelief was not analysed. The effect of creams on skin gloss was too important and could have interfered with the reconstruction of the 3D depth maps, leading to unreliable microrelief results.

Despite these limitations, it is interesting to note that the coefficients of variation obtained from repeatability studies of microrelief parameters on a single subject under controlled conditions are very similar to those obtained on the 17 subjects under nomadic conditions. On the cohort of subjects, these coefficients of variation are also within the same range when analysed using time points 30 min apart, indicating a good reproducibility within that time frame. Altogether, results are largely acceptable to produce a clear picture of the skin microrelief and validate the use of the connected camera to analyse the skin microrelief under real-life conditions. Results are sufficiently reliable to detect the already documented evolution of the microrelief with age. It has long been known that the patterning of the skin evolves with age,[34] and many works have confirmed it.[13,15–17,22,28,35,36] Collectively, they show that age correlates negatively with the number of furrows/plateaus while positively correlating with the depth and width of furrows. We obtained very similar results even if the limited cohort size and the very few elder subjects (only four over 45 years old) might have hindered us from highlighting all these changes.

A few minutes apart, results are reproducible while considering a single subject or the untreated zones of both forearms of the cohort. They are also reproducible within 8 h while analysing a stable model system. However, roughness and microrelief parameters show increased coefficients of variation over the 8 h of the study, revealing a variability of the skin roughness. Indeed, results show that microrelief evolved significantly during these 8 h leading to a rougher skin with a greater depth/height range and larger sectional areas of furrows/plateaus. If the link between the microrelief and skin roughness is quite obvious and documented,[19,36] intra-day variations in microrelief or skin roughness have not been pinpointed so far. A first explanation could be that intra-day variations in the intrinsic skin hydration affect *stratum corneum* characteristics, including its roughness.[37] Besides, several skin physiological parameters are under the control of day and night alternations, also called the circadian rhythm.[38–40] Among them are transepidermal water loss (TEWL) and the hydration of the *stratum corneum*.[41–43] If TEWL presents 8-, 12- and 24-h patterns with peaks in the morning and mid-afternoon, skin capacitance has an 8-h cycle with a maximum in the morning and smaller peaks at noon and mid-afternoon. Taken together, these findings could be a hypothesis for the observed alteration of the skin microrelief throughout the day. Indeed, in our case, the first acquisition (T0) was performed in the morning when skin hydration was at its highest, even for dry skins, resulting in a smoother skin. Eight hours later, in the late afternoon/early evening, skin appeared rougher which could reveal skin dehydration. The fact that the subjects recruited presented dry skin could have amplified the effect.

The microrelief reflecting the organisation of deeper cell layers and tissues,[5,10,19,44–47] and the circadian rhythm regulating many aspects of their physiology,[38–40] additional explanations could be invoked. Yet, the changes observed during the 8-h period could involve a totally different explanation, much more trivial and inherent to changes in environmental conditions. The study took place in winter and subjects spent their day in the office where the hot air from the heating system of the offices could have impacted skin hydration and roughness when dry.[20] Sorting out the relative importance of endogenous factors versus that of external influences is of interest. For doing so, a comparative analysis of results obtained under nomadic and controlled conditions should provide answers, especially if an enlarged group of subjects is examined to maximise the significance of results. Nevertheless, an important point of this study is that assessment of product performance was achieved by revealing slight but significant improvement of the microrelief by studying evolution over time relative to that of control areas.

Indeed, and contrary to the increase of the roughness/microrelief of the untreated skin areas during the 8 h of the study, those onto which a cream supplemented with moisturisers were applied led to smoother skin according to the global Ra, Rq and Spa parameters. As the placebo had almost no significant effect, the improvement of roughness/microrelief was due to the moisturiser. Yet, if all decrease the heterogeneity of roughness (Spa), only saccharide isomerate and xylitylglucoside–anhydroxylitol–xylitol led to a significant effect on the amplitude of the roughness. This difference might relate to the different nature of the moisturisers. Urea is a natural component of the moisturising factor (NMF). It is produced by the breakdown of protein or secreted by sebaceous and sweat glands.[48] When topically applied at low concentration, it reduces TEWL, improves hydration and water retention. The two other moisturisers are natural sugar derivatives. According to their manufacturers, both have a composition similar to that of the natural sugar fraction of the NMF, resulting in a strengthened barrier function and increased hydration of the *stratum corneum*. Still, they show some differences in their identified effects.

The decrease of skin roughness by moisturisers is also observed at the level of microrelief. This is significant for the height and the sectional surface of plateaus. Those two highly correlated parameters indicate a flattening of plateaus. In addition, there is a non-significant but strong trend in the reduction of the number of detected plateaus. This does not imply that they totally disappeared but, at least, that they became too shallow to be detected. This suggests a tendency to the levelling of plateaus. In fact, the application of moisturisers induces several non-statistically significant changes, which trends indicate a decreased roughness. It is possible that the combination of these non-significant changes, with the few significant ones, explains the impact observed on the Ra, Rq and Spa roughness parameters. Yet, effects are limited, possibly due to the short-term study we performed and the single product application. Indeed, substantiation claims showing an effect on skin texture often involve several days of repeated applications.

Nevertheless, results clearly indicate that the connected camera and its associated analysis software provide repeatable and reproducible microrelief results and are simple and reliable enough to be used for its evaluation by the subjects themselves while they are living their daily life. Under such nomadic conditions, it is possible to highlight

the age-related alteration of the microrelief. The improvement of skin smoothness upon moisturiser application links to a decreased roughness of the microrelief. This is the main benefit expected by consumers as it improves skin appearance.[49] They also reduce scaling induced by dry skin, bringing comfort as well as smoothness, and help compensate the altered barrier function of the *stratum corneum*.[50,51]

In addition to evaluating cosmetic formulae, results open up new fields of use for the connected camera. The possibility to detect age-related variations of the microrelief suggests that it can be used to study skin- and anti-ageing cosmetics. Other uses can be envisioned, such as monitoring moisturisers specifically developed for an age group, a specific population in its geographic zone, photoaged skin and so on. It also becomes possible to study the effect of specific environments. In our case, the study was carried out with office workers, but one could imagine analysing specific conditions subjects may endure and the effect of cosmetics under such situations. As these studies can be conducted under real conditions, their results should represent the actual effects of the environment or the performances of a cosmetic.

ACKNOWLEDGEMENTS

The authors wish to thank Dr Philippe Crouzet, Estium-Concept, for scientific writing services.

CONFLICT OF INTEREST

SG, TV, MC, EPM and MJ are the full-time employees of Newtone Technologies, a company specialised in the design of innovative solutions for skin imaging and analysis that set up the connected camera. EH, NC and EBV are the full-time employees of Seppic, a company developing and manufacturing ingredients for the cosmetic, pharmaceutic and veterinary industries. Seppic holds patents for a novel process of polyol-glycosides preparation and the topical use of xylitylglucoside–anhydroxylitol–xylitol as an agent improving human epidermis hydration.

FUNDING INFORMATION

The present study was co-funded by Newtone Technologies and Seppic.

DATA AVAILABILITY STATEMENT

The data that support the findings of this study are available from the corresponding author upon reasonable request.

REFERENCES

1. Serup J. EEMCO guidance for the assessment of dry skin (xerosis) and ichthyosis: clinical scoring systems. Skin Res Technol. 1995;1:109-114.
2. Brehler R, Voss W, Müller S. Glove powder affects skin roughness, one parameter of skin irritation. Contact Dermatitis. 1998;39:227-230.
3. Grove GL, Zerweck C, Pierce E. Noninvasive instrumental methods for assessing moisturizers. In: Leyden JJ, Rawlings AV, eds. Skin Moistuzation. Marcel Decker Inc, 2002:499-528.
4. Proksch E. Dryness in chronologically and photoaged skin. In: Loden M, Maibach HI, eds. Dry Skin and Moisturizers: Chemistry and Function. Vol. 1. 2nd ed. Taylor & Francis, 2006;117-126.
5. Hashimoto K. New methods for surface ultrastructure: comparative studies of scanning electron microscopy, transmission electron microscopy and replica method. Int J Dermatol. 1974;13:357-381.
6. Piérard-Franchimont C, Piérard GE. Assessment of aging and actinic damages by cyanoacrylate skin surface strippings. Am J Dermatopathol. 1987;9(6), 500-509.
7. Quatresooz P, Thirion L, Piérard-Franchimont C, Piérard GE. The riddle of genuine skin microrelief and wrinkles. Int J Cosmet Sci. 2006;28(6), 389-395.
8. Piérard GE, Franchimont C, Lapierre CM. Le vieillissement, son expression au niveau de la microanatomie et des propriétés physiques de la peau. Int J Cosmet Sci. 1980;2(4), 209-214.
9. Stamatas GN, Nikolovski J, Luedtke MA, Kollias N, Wiegand BC. Infant skin microstructure assessed *in vivo* differs from adult skin in organization and at the cellular level. Pediatr Dermatol. 2010;27(2),125-131.
10. Fischer TW, Wigger-Alberti W, Elsner P. Direct and non-direct measurement techniques for analysis of skin surface topography. Skin Pharmacol Appl Skin Physiol. 1999;12(1-2):1-11.
11. Chinn HD, Dobson RL. The topographic anatomy of human skin. Arch Dermatol. 1964;89:267-273.
12. Corcuff P, Lévêque JL, Grove GL, Kligman AM. The impact of aging on the microrelief of peri-orbital and leg skin. J Soc Cosmet Chem. 1987;82:145-152.
13. Manuskiatti W, Schwindt DA, Maibach HI. Influence of age, anatomic site and race on skin roughness and scaliness. Dermatology. 1998;196:401-407.
14. Akazaki S, Nakagawa H, Kazama H, et al. Age-related changes in skin wrinkles assessed by a novel three-dimensional morphometric analysis. Br J Dermatol. 2002;147:689-695.
15. Jacobi U, Chen M, Frankowski G, et al. *In vivo* determination of skin surface topography using an optical 3D device. Skin Res Technol. 2004;10:207-214.
16. Lagarde JM, Rouvrais C, Black D. Topography and anisotropy of the skin surface with ageing. Skin Res Technol. 2005;11:110-119.
17. Li L, Mac-Mary S, Marsaut D, et al. Age-related changes in skin topography and microcirculation. Arch Dermatol Res. 2006;297:412-416.
18. Corcuff P, Francois AM, Lévêque JL, Porte G. Microrelief changes in chronically sun-exposed human skin. Photodermatol Photoimmunol Photomed. 1988;5:92-95.
19. De Paepe K, Lagarde JM, Gall Y, Roseeuw D, Rogiers V. Microrelief of the skin using a light transmission method. Arch Dermatol Res. 2000;292:500-510.
20. Egawa M, Oguri M, Kuwahara T, Takahashi M. Effect of exposure of human skin to a dry environment. Skin Res Technol. 2002;8:212-218.
21. Corcuff P, de Rigal J, Lévêque JL, Makki S, Agache P. Skin relief and ageing. J Soc Cosmet Sci. 1983;34:177-190.
22. Vörös E, Robert C, Godeau G, Robert AM. Morphometric study of the evolution of the skin surface relief with age. Acta Stereol. 1989;8:379-380.
23. Lévêque JL, Querleux B. SkinChip®, a new tool for investigating the skin surface *in vivo*. Skin Res Technol. 2003;9:343-347.
24. Tchvialeva L, Zeng H, Markhvida I, McLean DI, Lui H, Lee T. Skin roughness assessment. In: Campolo D, ed. New Developments in Biomedical Engineering. IntechOpen Limited, 2010;341-358.
25. Bontozoglou C, Zhang X, Xiao P. Micro-relief analysis with skin capacitive imaging. Skin Res Technol. 2019;25:165-170.
26. Kottner J, Schario M, Bartels NG, Pantchechnikova E, Hillmann K, Blume-Peytavi U. Comparison of two *in vivo* measurements for skin surface topography. Skin Res Technol. 2013;19:84-90.
27. Tronnier H, Wiebusch M, Heinrich U, Stute R. Surface evaluation of living skin. Adv Exp Med Biol. 1999;455:507-516.
28. Messaraa C, Metois A, Walsh M, et al. Wrinkle and roughness measurement by the Antera 3D and its application for evaluation of cosmetic products. Skin Res Technol. 2018;24:359-366.
29. Constantin MM, Poenaru E, Poenaru C, Constantin T. Skin hydration assessment through modern non-invasive bioengineering technologies. Maedica. 2014;9:33-38.

30. Hertzmann A, Seitz SM. Shape and materials by example: a photometric stereo approach. Proc. 2003 IEEE Computer Society Conference on Computer Vision and Pattern Recognition. 2003;1:533-540.
31. Hertzmann A, Seitz SM. Example-based photometric stereo: shape reconstruction with general, varying BRDFs. IEEE Trans Pattern Anal Mach Intell. 2005;27:1254-1264.
32. Santo H, Samejima M, Matsushita Y. Numerical shape-from-shading revisited. IPSJ Trans Comput Vis Appl. 2018;10:8.
33. Bae EJ, Seo SH, Kye YC, Ahn HH. A quantitative assessment of the human skin surface using polarized light digital photography and its dermatologic significance. Skin Res Technol. 2010;16:270-274.
34. Lavker RM, Kwong F, Kligman AM. Changes in skin surface patterns with age. J Gerontol. 1980;35:348-354.
35. Masuda Y, Oguri M, Morinaga T, Hirao T. Three-dimensional morphological characterization of the skin surface micro-topography using a skin replica and changes with age. Skin Res Technol. 2014;20:299-306.
36. Trojahn C, Dobos G, Schario M, Ludriksone L, Blume-Peytavi U, Kottner J. Relation between skin micro-topography, roughness, and skin age. Skin Res Technol. 2015;21:69-75.
37. Dabrowska AK, Adlhart C, Spano F, et al. *In vivo* confirmation of hydration-induced changes in human-skin thickness, roughness and interaction with the environment. Biointerphases. 2016;11:031015.
38. Plikus MV, Van Spyk EN, Pham K, et al. The circadian clock in skin: implications for adult stem cells, tissue regeneration, cancer, aging, and immunity. J Biol Rhythms. 2015;30:163-182.
39. Matsui MS, Edward Pelle E, Dong K, Pernodet N. Biological rhythms in the skin. Int J Mol Sci. 2016;17:801.
40. Lyons AB, Moy L, Moy R, Tung R. Circadian rhythm and the skin: a review of the literature. J Clin Aesthet Dermatol. 2019;12:42-45.
41. Reinberg AE, Touitou Y, Soudant E, Bernard D, Bazin R, Mechkouri M. Oral contraceptives alter circadian rhythm parameters of cortisol, melatonin, blood pressure, heart rate, skin blood flow, transepidermal water loss, and skin amino acids of healthy young women. Chronobiology. 1996;13:199-211.
42. Yosipovitch G, Xiong GL, Haus E, Sackett-Lundeen L, Ashkenazi I, Maibach HI. Time-dependent variations of the skin barrier function in humans: transepidermal water loss, stratum corneum hydration, skin surface pH, and skin temperature. J Invest Dermatol. 1998;110:20-23.
43. Le Fur I, Reinberg A, Lopez S, Morizot F, Mechkouri M, Tschachler E. Analysis of circadian and ultradian rhythms of skin surface properties of face and forearm of healthy women. J Invest Dermatol. 2001;117:718-724.
44. Matsunga N, Itcho K, Hamamura K, et al. 24-hour rhythm of aquaporin-3 function in the epidermis is regulated by molecular clocks. J Invest Dermatol. 2014;134:1636-1644.
45. Jaspers S, Hopermann H, Sauermann G, Hoppe U, Lunderstädt R, Ennen J. Rapid *in vivo* measurement of the topography of human skin by active image triangulation using a digital micromirror device. Skin Res Technol. 1999;5:195-207.
46. Fenske NA, Lober CW. Structural and functional changes of normal aging skin. J Amer Acad Dermatol. 1986;15:571-585.
47. Piérard GE. EEMCO guidance to the *in vivo* assessment of tensile functional properties of the skin. Part 1: Relevance to the structures and ageing of the skin and subcutaneous tissues. Skin Pharmacol Appl Skin Physiol. 1999;12:352-362.
48. Celleno L. Topical urea in skincare: a review. Dermatol Ther. 2018;31:e12690.
49. Jiang ZX, DeLaCruz J. Appearance benefits of skin moisturization. Skin Res Technol. 2011;17:51-55.
50. Purnamawati S, Indrastuti N, Danarti R, Saefudin T. The role of moisturizers in addressing various kinds of dermatitis: a review. Clin Med Res. 2017;15:75-87.
51. Draelos ZD. The science behind skin care: moisturizers. J Cosmet Dermatol. 2018;17:138-144.

How to cite this article: Gougeon S, Hernandez E, Chevrot N, et al. Evaluation of a new connected portable camera for the analysis of skin microrelief and the assessment of the effect of skin moisturisers. Skin Res Technol. 2023;29:1–15. https://doi.org/10.1111/srt.13190